Improving dimensional accuracy by error modelling and its compensation for 3-axis Vertical Machining Centre

H M Dobariya[1], Y D Patel[2], D A Jani[3]

Abstract

In today's era, machining centres are very important units of manufacturing systems. Due to the structural characteristics, inaccuracy of the tool tip position is inherent. This could be a result of geometric error, thermal error, fixture dependant error and cutting force induced error. The geometric error contributes 70% of the total errors related to a machine tool. Present work focuses on improving dimensional accuracy of a 3-axis vertical machining centre (VMC). Accurate error estimation in machine tools is possible using kinematic error model. Initially, kinematic model for an error free VMC with TTT configuration was developed using D-H convention. Subsequently, a kinematic error model was developed by same technique considering 12 geometric error components. The actual error measurement along each axis was carried out using 3D microscope and vernier depth gauge. The concept of interpolation function was used to predict error distribution in a workspace enclosure. An error compensation algorithm using predicted error was developed and was also validated experimentally.

Keywords: Kinematic modelling of 3-axis VMC, Geometric error model, Prediction of error distribution and Compensation.

1 Introduction

Dimensional accuracy of a machined component is one of the most important and critical parameter in determining the quality of machined component. Dimensional accuracy of a component machined using CNC machines, is largely affected by factors like cutting tool and machining conditions, resolution of the machine tool, type of workpiece. Performance consistency of a machine tool depends on its ability to accurately position the tool tip.

The difference between the actual positions achieves by the tool tip and the commanded position of the tool tip is known as position error. The machining condition and environment will affects the error generated. Always some error remains present, once some of the factors are keeping fixed at some extent. The gradually wear of components of drive system and the manufacturing defects occurs in major components related to the axis travel are dominants responsible for erroneous position of tool.

The actual position achieved by the tool is defined by the sum of commended position and the error at the commended position. Let, commended position P, the actual position achieved by the tool is P_a, and then the error at the commended position is given by the following Eq. (1):

$$E_P = P - P_a \qquad (1)$$

---

[1] A D Patel Institute of Technology (ADIT), New V. V. Nagar-388121, hmdobariya@gmail.com
[2] Department of Mechanical Engineering, ADIT, New V. V. Nagar-388121, yash523@rediffmail.com
[3] Department of Mechanical Engineering, ADIT, New V. V. Nagar-388121, dhaval.jani@gmail.com

Where,

P = Desired tool position
P_a = Actual tool position
E_P = Error at point P

Geometric error related to a machine tool structure contributes 70% of total errors as reported by Kiridena and Ferreira [1]. The geometric error varies slowly with time, and thus it is advantageous to compensate this error compared to other errors. Kiridena and Ferreira [1] developed a kinematic error model for five axis milling machine using D-H convention. They also derived nth order quasi-static error model for 3-axis VMC using shape and joint transformation [2].

Chen et al. [3] developed quasi-static error model with non- linear behaviour using rigid body kinematic approach for multi axis CNC machining centres. Rahman et al. [4] have presented a geometric error model using homogeneous transformation for a three axis horizontal machine tool. Laser interferometer and double ball bar were used for error measurement of machine tool. A kinematic error model of geometric and thermal errors using rigid body kinematic approach was reported by Okafor et al. [5]. They have defined the positional error along each axes as a component of resultant volumetric error. Soori et al. [6, 7] formulated a kinematic error model with geometric, cutting force and tool deflection errors for a three axis milling machine. A kinematic error model for RRTTT configuration of five axis VMC was prepared using the D-H convention by Talyan et al. [8].

The general methodology used by the researchers to compensate the error consists of three steps:

1. Development of kinematic error model of machine tool
2. Measurement of errors in workspace
3. Development of compensation algorithm

It was found that the kinematic modelling of 3-axis vertical machining centre using D-H convention is not reported. Therefore, the present work emphasis upon kinematic modelling of a 3-axis VMC and prediction of error distribution using 1D element in workspace enclosure along with its offline compensation.

2 Kinematic Modelling of 3-axis VMC of without Error

Kinematic model of machine tool is a mathematical representation for deviation of motion along each axis, imperfect position, dimensions and alignment of the structural members on the basis of geometric errors. In kinematic modelling of machine tool using D-H convention, it is necessary to assign coordinate transformation frames at each important location of machine tool. Schematic diagram of a typical 3-axis VMC and its equivalent kinematic model is shown in Fig. (1) and Fig. (2) respectively.

The fixed programming coordinate frame $\mathrm{C_f}$ with respect to which part programming for CNC machine is referred. Probe coordinate frame $\mathrm{C_p}$, is defined at the center of the spherical probe as in case of touch trigger probe as shown in Fig. (2). Target point coordinate frame $\mathrm{C_x}$, is used to map the target point with reference to the fixed programming coordinate frame. Cutting point coordinate frame is located at the cutting point on the tool relative to probe coordinate frame.

Here, notation used in kinematic modelling are listed as below.

$a_i,\ b_i, c_i$ = Nominal dimensions of machine elements along X, Y and Z axis respectively
x_i = Displacement of joint i

$X_i =$ Coordinates of the target point, i=1, 2, 3 for X, Y and Z axis respectively.

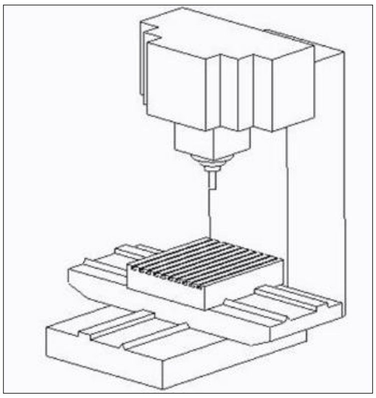

Figure 1: Schematic diagram of a typical 3-axis VMC

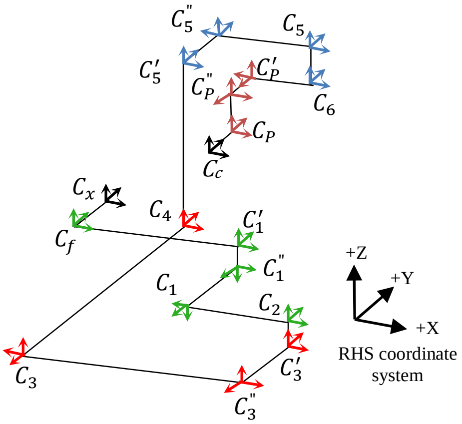

Figure 2: Kinematic equivalent of 3-axis VMC

The translation from fixed programming to target point coordinate frame is denoted by $\mathrm{T_{tp}}$. The transformation matrices from $\mathrm{T_0}$ to $\mathrm{T_{15}}$ between fixed programming and probe coordinate frame were obtained using D-H parameters as per Table 1.

Table 1: D-H parameters of transformation for 3-axis VMC without error

$Transformation$ $matrix$	$Between$ $Frames$	$D-H\ Parameters$			
		θ	d	a	α
T_0	$C_f - C_1'$	$-$	$-$	a_1	$-$
T_1	$C_1' - C_1^{"}$	$-$	c_1	$-$	180
T_2	$C_1^{"} - C_1$	90	$-$	$-b_1$	$-$
T_3	$C_1 - C_2$	-90	$-$	x_1	180
T_4	$C_2 - C_3'$	$-$	c_2	$-$	$-$
T_5	$C_3' - C_3^{"}$	-90	$-$	$-b_2$	$-$
T_6	$C_3^{"} - C_3$	-90	$-$	$-a_2$	$-$
T_7	$C_3 - C'_4$	-90	$-$	x_2	$-$
T_8	$C'_4 - C_4$	-90	$-$	$-$	$-$
T_9	$C_4 - C_5'$	$-$	c_3	$-$	$-$
T_{10}	$C_5' - C_5^{"}$	90	$-$	b_3	$-$
T_{11}	$C_5^{"} - C_5$	-90	$-$	a_3	$-$
T_{12}	$C_5 - C_6$	$-$	x_3	$-$	$-$
T_{13}	$C_6 - C_p'$	180	$-$	$-a_4$	$-$
T_{14}	$C_p' - C_p^{"}$	90	$-$	b_4	$-$
T_{15}	$C_p^{"} - C_p$	90	c_4	$-$	$-$

The translation along X-axis (T_x), Y-axis (T_y) and Z-axis (T_z) are defined by frames $\mathrm{C_f}$ to $\mathrm{C_2}$, $\mathrm{C_2}$ to $\mathrm{C_4}$ and $\mathrm{C_4}$ to $\mathrm{C_6}$ respectively as shown in Fig. (2). The transformation up to the probe coordinate frame can be described by frames $\mathrm{C_6}$ to $\mathrm{C_p}$. The transformation for cutting point $(-a_t, -b_t, -c_t)$ with respect to the probe coordinate frame is expressed by $\mathrm{T_c}$.

The resulting transformation from target point to cutting point coordinate frame can be obtained by multiplying the transformation matrices in sequence. Both frames must be coincide for VMC without error to obtain a closed loop kinematic chain as shown by Eq. (2). The final transformation matrix is expressed in such case by Eq. (3). The obtained results were same as reported using concept of shape and joint transformation matrix by Kiridena and Ferreira [2] for same configuration machine tool.

$$\left[\boldsymbol{T_{tp}}\right]\cdot\left[\boldsymbol{T_x}\right]\cdot\left[\boldsymbol{T_y}\right]\cdot\left[\boldsymbol{T_z}\right]\cdot\left[\boldsymbol{T_p}\right]\cdot\left[\boldsymbol{T_c}\right]=\left[\boldsymbol{I}\right] \tag{2}$$

$$\begin{bmatrix} \mathbf{1} & \mathbf{0} & \mathbf{0} & \boldsymbol{a_1+a_2+a_3+a_4+x_1+X_1+a_t} \\ \mathbf{0} & \mathbf{1} & \mathbf{0} & \boldsymbol{b_1+b_2+b_3+b_4+x_2+X_2+b_t} \\ \mathbf{0} & \mathbf{0} & \mathbf{1} & \boldsymbol{c_1+c_2+c_3+c_4+x_3+X_3+c_t} \\ \mathbf{0} & \mathbf{0} & \mathbf{0} & \mathbf{1} \end{bmatrix}=\left[\boldsymbol{I}\right] \tag{3}$$

3 Development of Kinematic Error Model

The kinematic error model for a machine tool is used to describe the relationship between individual error components and its effect on overall position. The closed loop kinematic chain cannot be achieved for inaccurate machine tool resulting in a non-coincidence of target point and cutting point coordinate frames. Many researchers have established error model using different error considerations as reported in literature [2-8] for machine tools.

Twelve components of geometric error (viz. 3 each for straightness, flatness, squareness and scale (linear positional error) error along X, Y and Z axis respectively) requires more attention among 21 components. The error components present in X-axis slide are illustrated in Fig. (3).

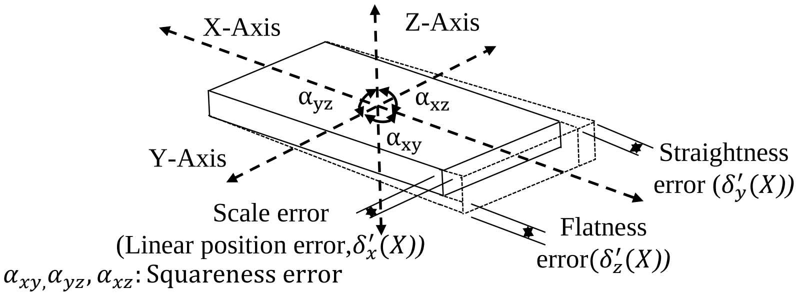

Figure 3: Geometric error components related to X-axis slide

These error components on kinematic chain of machine tool with dark colour lines are shown in Fig. (4(a)). The location for coordinate frames are indicated in Fig. (4(b)).

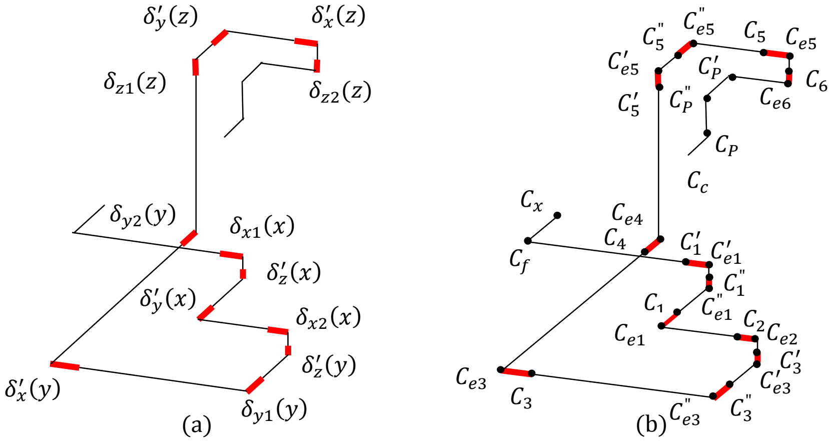

Figure 4: (a) Geometric error components (b) Location of coordinate transformation frames on kinematic chain of 3-axis VMC

The transformation along error components e.g. from coordinate transformation frame at original position (C'_1) to erroneous position (C'_{e1}) is only translation. Therefore, coordinate transformation frame with same orientation are used at both these location. Here, erroneous distance can be directly added or subtracted into the original positional distance.

Here, $\delta_{i1}(i)$ = Scale error in i-axis travel slide in i direction
$\delta_{i2}(i)$ = Positional error in recirculating ball screw of i-travel
α_{ij} = Squareness error between i and j axis slide Where, i, j= X, Y and Z
$\delta'_y(x), \delta'_x(y), \delta'_x(z)$ = Straightness error in X, Y and Z axis travel slide in Y, X and X direction respectively.
$\delta'_z(x), \delta'_z(y), \delta'_y(z)$ = Flatness error in X, Y and Z axis travel slide in Z, Z and Y direction respectively.

- **Translation along X-axis:**

Geometric error along any axis slide is mainly due to dimensional deviation and erroneous motion of recirculating ball screw. The transformation matrices T_{E0} to T_{E3} were obtained from D-H parameters of kinematic error model as per Table 2.

The final transformation matrix for machine tool slide along X-axis with error was obtained by post-multiplying sub-transformations matrices in sequence as per Eq. (4).

$$\boldsymbol{T_{Ex} = T_{E0} \cdot T_{E1} \cdot T_{E2} \cdot T_{E3}} \tag{4}$$

$$= \begin{bmatrix} \mathbf{1} & \mathbf{0} & \mathbf{0} & \boldsymbol{a_1 + x_1 + \delta_{x1}(x) + \delta_{x2}(x)} \\ \mathbf{0} & \mathbf{1} & \mathbf{0} & \boldsymbol{b_1 + \delta_y(x)} \\ \mathbf{0} & \mathbf{0} & \mathbf{1} & \boldsymbol{c_1 + \delta_z(x)} \\ \mathbf{0} & \mathbf{0} & \mathbf{0} & \mathbf{1} \end{bmatrix} \tag{5}$$

Error due to manufacturing defect $\delta_{x1}(x)$, positional error of recirculating ball screw $\delta_{x2}(x)$, straightness error $\delta_y(x)$and flatness error $\delta_z(x)$ are of X-axis slide [5] as shown in Fig. (3) and are expressed by Eq. (6-8).

$$\delta_x(x) = \delta_{x1}(x) + \delta_{x2}(x) \tag{6}$$

$$\delta_y(x) = \delta'_y(x) + \alpha_{xy} \cdot x_1 \tag{7}$$

$$\delta_z(x) = \delta'_z(x) + \alpha_{xz} \cdot x_1 \tag{8}$$

Table 2: D-H parameters for kinematic error model

$Matrix$	$Between\ frames$	$D-H\ Parameters$			
		θ	d	a	α
T_{E0}	$C_f - C'_{e1}$	$-$	$-$	$a_1 + \delta_{x1}(x)$	$-$
T_{E1}	$C'_{e1} - C''_{e1}$	$-$	$c_1 + \delta_z(x)$	$-$	180
T_{E2}	$C''_{e1} - C_{e1}$	90	$-$	$-b_1 - \delta_y(x)$	$-$
T_{E3}	$C_{e1} - C_{e2}$	-90	$-$	$x_1 + \delta_{x2}(x)$	180
T_{E4}	$C_{e2} - C'_{e3}$	$-$	$c_2 + \delta_z(y)$	$-$	$-$
T_{E5}	$C'_{e3} - C''_{e3}$	-90	$-$	$-b_2 - \delta_{y1}(y)$	$-$
T_{E6}	$C''_{e3} - C_{e3}$	-90	$-$	$-a_2 - \delta_x(y)$	$-$
T_{E7}	$C_{e3} - C'_{e4}$	-90	$-$	$x_2 + \delta_{y2}(y)$	$-$
T_{E8}	$C'_{e4} - C_{e4}$	-90	$-$	$-$	$-$
T_{E9}	$C_{e4} - C'_{e5}$	$-$	$c_3 + \delta_{z1}(z)$	$-$	$-$
T_{E10}	$C'_{e5} - C''_{e5}$	90	$-$	$b_3 + \delta_y(z)$	$-$
T_{E11}	$C''_{e5} - C_{e5}$	-90	$-$	$a_3 + \delta_x(z)$	$-$
T_{E12}	$C_{e5} - C_{e6}$	$-$	$x_3 + \delta_{z2}(z)$	$-$	$-$

Similarly, the same procedure is used for determining Y and Z axis translation and matrices for the same are shown by Eq. (9) and (10). The transformation up to the probe coordinate frame, C_p can be expressed using Eq. (11).

$$\boldsymbol{T_{Ey}} = \begin{bmatrix} \mathbf{1} & \mathbf{0} & \mathbf{0} & \boldsymbol{a_2 + \delta_x(y)} \\ \mathbf{0} & \mathbf{1} & \mathbf{0} & \boldsymbol{b_2 + x_2 + \delta_{y1}(y) + \delta_{y2}(y)} \\ \mathbf{0} & \mathbf{0} & \mathbf{1} & \boldsymbol{c_2 + \delta_z(y)} \\ \mathbf{0} & \mathbf{0} & \mathbf{0} & \mathbf{1} \end{bmatrix} \tag{9}$$

$$\boldsymbol{T_{Ez}} = \begin{bmatrix} \mathbf{1} & \mathbf{0} & \mathbf{0} & \boldsymbol{a_3 + \delta_x(z)} \\ \mathbf{0} & \mathbf{1} & \mathbf{0} & \boldsymbol{b_3 + \delta_y(z)} \\ \mathbf{0} & \mathbf{0} & \mathbf{1} & \boldsymbol{c_3 + x_3 + \delta_{z1}(z) + \delta_{z2}(z)} \\ \mathbf{0} & \mathbf{0} & \mathbf{0} & \mathbf{1} \end{bmatrix} \tag{10}$$

$$\boldsymbol{T_{Ep}} = \boldsymbol{T_{E13}} \cdot \boldsymbol{T_{E14}} \cdot \boldsymbol{T_{E15}} = \begin{bmatrix} \mathbf{1} & \mathbf{0} & \mathbf{0} & \boldsymbol{a_4} \\ \mathbf{0} & \mathbf{1} & \mathbf{0} & \boldsymbol{b_4} \\ \mathbf{0} & \mathbf{0} & \mathbf{1} & \boldsymbol{c_4} \\ \mathbf{0} & \mathbf{0} & \mathbf{0} & \mathbf{1} \end{bmatrix} \tag{11}$$

The transformation from target point to cutting point coordinate frame are defined by Eq. (12) due to open loop kinematic chain. If the transformation between these two coordinate frames is [R], then

$$[\boldsymbol{T_{Etp}}] \cdot [\boldsymbol{T_{Ex}}] \cdot [\boldsymbol{T_{Ey}}] \cdot [\boldsymbol{T_{Ez}}] \cdot [\boldsymbol{T_{Ep}}] \cdot [\boldsymbol{T_{Ec}}] = [\boldsymbol{R}] \tag{12}$$

$$\begin{bmatrix} \mathbf{1} & \mathbf{0} & \mathbf{0} & \boldsymbol{a_1 + a_2 + a_3 + a_4 + x_1 + X_1 + a_t + E'_x} \\ \mathbf{0} & \mathbf{1} & \mathbf{0} & \boldsymbol{b_1 + b_2 + b_3 + b_4 + x_2 + X_2 + b_t + E'_y} \\ \mathbf{0} & \mathbf{0} & \mathbf{1} & \boldsymbol{c_1 + c_2 + c_3 + c_4 + x_3 + X_3 + c_t + E'_z} \\ \mathbf{0} & \mathbf{0} & \mathbf{0} & \mathbf{1} \end{bmatrix} = [\boldsymbol{R}] \tag{13}$$

$$Where, \qquad E'_i = \delta_i(x) + \delta_i(y) + \delta_i(z), \qquad i = x, y, z \tag{14}$$

These components represents the positional error along X, Y and Z axis. The positional vector [E] for geometric error model is same as reported in [2],

$$[\boldsymbol{E}] = [\boldsymbol{R}] \cdot \begin{bmatrix} \mathbf{0} \\ \mathbf{0} \\ \mathbf{0} \\ \mathbf{1} \end{bmatrix} \tag{15}$$

$$\therefore \begin{bmatrix} \boldsymbol{E_x} \\ \boldsymbol{E_y} \\ \boldsymbol{E_z} \\ \boldsymbol{1} \end{bmatrix} = \begin{bmatrix} \boldsymbol{a_1 + a_2 + a_3 + a_4 + x_1 + X_1 + a_t + E'_x} \\ \boldsymbol{b_1 + b_2 + b_3 + b_4 + x_2 + X_2 + b_t + E'_y} \\ \boldsymbol{c_1 + c_2 + c_3 + c_4 + x_3 + X_3 + c_t + E'_z} \\ \boldsymbol{1} \end{bmatrix} \tag{16}$$

The elements E_x, E_y and E_z are positional components along X, Y and Z axis, which indicate the amount through which tool has to move for target point on machining component. This kinematic error model for machine tool structure is helpful to obtain the positional error components along each axis.

4 Error Measurement

It is necessary to measure the error along each axis of VMC at various points in workspace for error distribution prediction. In present work, error measurement of machined components on 3-axis VMC are carried out using 3D microscope and vernier depth gauge along each axis as shown in Fig. (5). The 3D microscope of 0.01 µm resolution and vernier depth gauge with 0.01 mm least count are used here. The positional errors are summarized in Table 3.

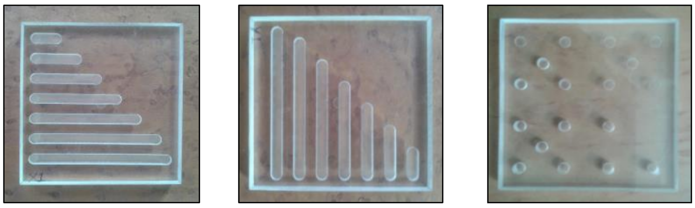

Figure 5: Machined components for X, Y and Z axis error measurement respectively

Table 3: Actual error along axes in 3-axis VMC (All dimensions are in µm)

Axis	*Min. error*	*Max. error*	*Mean error*	*Error distribution*
X	*5*	*363*	*96*	*Linear*
Y	*90*	*539*	*250*	*Linear*
Z	*-17*	*38*	*63*	*Quadrati c*

4.1 Prediction of error distribution

The prediction of error distribution in workspace are important to mimic the approximate behaviour of error in workspace. The meshing concept of FEM are used to discretise the workspace enclosure into finite number of elements. The actual error measured at some limited points are the base of error prediction.

Chen et al. [3] and Wang et al. [9] have worked with 3-D hexahedron element to predict the error in workspace. In 3-D hexahedron element, it is very difficult to include different error distribution i.e. linear and quadratic error distribution along the separate axis. The work using 3-D hexahedron element is efficient only when same types of error distribution exist along all the axis in workspace. However it seen that, the different cases may exist for linear and quadratic distribution along various axis of machine tool. It may also possible that either error does not exist in every axis of machine tool or each axis follow the different error distribution i.e. linear or quadratic distribution. These different cases are considered after error measurement of the machine tool.

It is very simple to map error distribution along separate axis with 1-D linear and quadratic element as in case of our machine tool where X and Y axis follow linear and Z axis follow quadratic error distribution. The compensation scheme can be implemented after determining the error distribution along respective axis.

5 Error compensation

Compensation can be implemented through modified G-codes, using piezoelectric ceramic brake compensation method, and external coordinate offset compensation method as reported by Fan et al. [10]. The concept of interpolation was employed to mimic erroneous behaviour of workspace in pre-calibrated error compensation technique. Here, modification of hardware is not required. This technique is implemented by modifying NC part program and it is employed for repetitive machining of large number of parts manufactured on the same machine tool.

Chen et al. [3] and Wang et al. [9] carried out an error compensation from predicted error using hexahedron element. Rahman et al. [4] developed the two software based correction ways for error compensation by counting new axes values by: (i) Post processor (PP) and (ii) Extra NC program processor (ENPP). The volumetric error compensation values were calculated from multiple regression analysis and ANN approach by Okafor and Ertekin [5]. Visual programming language was used by Soori et al. [6, 7] for the development of error compensation software. Talyan et al. [8] have used offline error compensation by modifying the NC program from the error model developed.

In the present work, the offline error compensation techniques was employed using the modification of NC part program through the C/C++ program. The error distribution in workspace is helpful to obtain the corrected points along the path of tool. The compensation of positional error was validated experimentally.

5.1 Algorithm of error compensation

The modified NC part program file will be generated according to the error distribution of each axis separately as per requirement with in workspace. The modification in X, Y and Z coordinate of each positions of the tool path was operated in NC part program file using C/C++ software. The flowchart is developed for position error compensation as shown in Fig. (6).

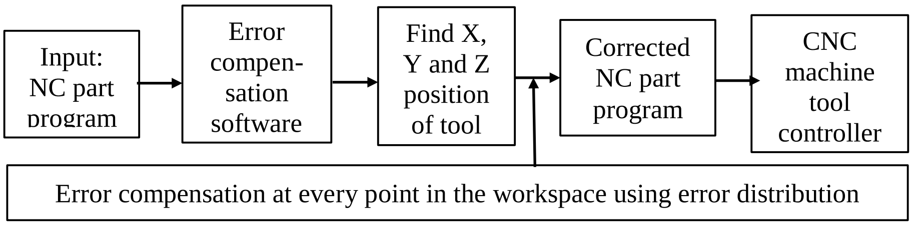

Figure 6: Flowchart of error compensation

5.2 Experimental work

The experiments were conducted with Acrylic component of (80×80×10) mm size and end mill cutter of 5 mm diameter on a 3-axis VMC. The experimental setup is shown in Fig. (7).The machined components with known patterns were prepared as shown in Fig. (8), to validate the effect of error compensation along X-axis. The measurement of machined components were carried out with a 3D microscope.

Machining of component was carried out with the original NC part program as well as error compensated NC part program. Here, the compensation of error along X-axis is focussed as shown in Fig (8). The errors in the linear distance along X-axis along with the improvement in result of errors are mentioned in Table 4. The experimental result shows the improvement of error compensation up to 67%. The same procedure was used for all the axis simultaneously.

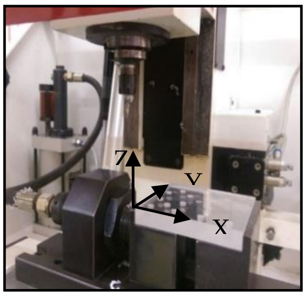

Figure 7: Experimental setup on 3-axis VMC

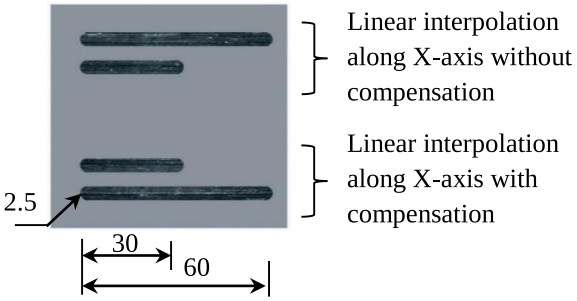

Figure 8: Geometry for X-axis travel machined component (All dimensions are in mm)

Table 4: Experimental results for 3-axis VMC (All dimensions are in mm)

Original length	*Measured length*	*Error before compensation*	*Measured length with error compensation*	*Error after compensation*
30	*29.7177*	*-0.2823*	*29.9384*	*-0.0616*
60	*60.0690*	*0.0690*	*60.0315*	*0.0315*

6 Conclusion

This paper presents the kinematic error modelling of 3-axis VMC with 12 most influencing geometric error components using D-H convention. The 3D microscope and vernier depth gauge were used to measure the error along each slides. One dimensional element for each axis separately is suggested for prediction of error distribution in workspace rather than hexahedron element. This will become more beneficial in case of different error distribution along each axis. At last the offline error compensation through the modifying NC part program was carried out. The predicted error distribution are used in the compensation of error using developed C/C^{++} program. The experimental result shows 67% improvement in the error.

References

[1] V. S. B. Kiridena, P. M. Ferreira, “Mapping the effects of positioning errors on the volumetric accuracy of five-axis CNC machine tools”, International Journal of Machine Tools and Manufacture, Vol. 33, pp. 417-437, 1993.

[2] V. S. B. Kiridena, P. M. Ferreira, “Kinematic modelling of quasi-static errors of three-axis machining centres”, International Journal of Machine Tools Manufacture, Vol. 34, pp. 85-100, 1994.

[3] X.B. Chen, A. Geddam and Z.J. Yuan, “Accuracy improvement of three axis CNC machining centers by quasi static error compensation”, Journal of manufacturing systems, Vol. 16, pp. 323-336, 1997.

[4] Mahbubur Rahman, Jouko Heikkala and Kauko Lappalainen, “Modelling, measurement and error compensation of multi-axis machine tools Part I theory”, International Journal of Machine Tools and Manufacture, Vol. 40, pp. 1535-1546, 2000.

[5] A.C.Okafor and Yalcin M. Ertekin, “Derivation of machine tool error models and error compensation procedure for three axes vertical machining center using rigid body kinematics”, International Journal of Machine Tools and Manufacture, Vol. 40, pp. 1199-1213, 2000.

[6] Mohsen Soori, Behrooz Arezoo and Mohsen Habibi, “Virtual machining considering dimensional, geometrical and tool deflection errors in three-axis CNC milling machines”, Journal of manufacturing systems, 2014.

[7] Mohsen Soori, Behrooz Arezoo and Mohsen Habibi, “Dimensional and geometrical errors of three-axis CNC milling machines in virtual machining system”, Computer Aided Design, Vol. 45, pp. 1306-1313, 2013.

[8] Akash Talyan, Anik Manglik, Rukhsar Hussain, Anita Singh,Tulika Varshney and Binit Kumar Jha,” Error Compensation and Accuracy Improvement in Five-Axis CNC Machine tool”, International Journal of Advanced Mechanical Engineering, Vol. 4, pp. 129-138, 2014.

[9] Shih-Ming Wang, Yuan-Liang Liu and Yuan Kang, “An efficient error compensation system for CNC multi-axis machines”, International Journal of Machine Tools and Manufacture, Vol. 42, pp. 1235-1245, 2002.

[10] Kaiguo Fan, Jianguo Yang and Liyan Yang, “Unified error model based spatial error compensation for four types of CNC machining center: Part-I Singular function based unified error model”, Mechanical Systems and Signal Processing, 2015.